SAND2015-2157C

Proceedings of the 9th International Conference on Energy Sustainability
ES2015
June 28 – July 2, 2014, San Diego, California, USA

PowerEnergy2015-49431

NOVEL TUBULAR RECEIVER PANEL CONFIGURATIONS FOR INCREASED EFFICIENCY OF HIGH-TEMPERATURE SOLAR RECEIVERS

Joshua M. Christian
Sandia National Laboratories, Concentrating Solar Technologies Department
Albuquerque, NM 87185-1127, USA.

Jesus D. Ortega
Sandia National Laboratories, Concentrating Solar Technologies Department
Albuquerque, NM 87185-1127, USA.

Clifford K. Ho
Sandia National Laboratories,
Concentrating Solar
Technologies Department
Albuquerque, NM 87185-1127,
USA.

ABSTRACT

Typical Concentrated Solar Power (CSP) central receiver power plants require the use of either an external or cavity receiver. Previous and current external receivers consist of a series of tubes connected to manifolds that form a cylindrical or rectangular shape such as in the cases of Solar One, Solar Two, and most recently the Ivanpah solar plant. These receivers operate at high surface temperatures (>600°C) at which point thermal re-radiation is significant. However, the geometric arrangement of these heat transfer tubes results in heat losses directly to the environment. This work focused on how to fundamentally reduce this heat loss through the manipulation of heat transfer tube configurations. Four receiver configurations are studied: flat receiver (base case study), a radial receiver with finned structures (fins arranged in a circular pattern on a cylinder), a louvered finned structure (horizontal and angled fins on a flat plate), and a vertical finned structure (fins oriented vertically along a flat plate). The thermal efficiency, convective heat loss patterns, and air flow around each receiver design is found using the computational fluid dynamics (CFD) code ANSYS FLUENT. Results presented in this paper show that alternative tubular configurations increase thermal efficiency by increasing the effective solar absorptance of these high-temperature receivers by increasing the light trapping effects of the receiver, reducing thermal emittance to the environment, and reducing the overall size of the receiver. Each receiver configuration has finned structures that take advantage of the directional dependence of the heliostat field resulting in a light trapping effect on the receiver. The finned configurations tend to lead to "hot" regions on the receiver, but the new configurations can take advantage of high local view factors (each surface can "see" another receiver surface) in these regions through the use of heat transfer fluid (HTF) flow patterns. The HTF reduces the temperatures in these regions increasing the efficiency of heat transfer to the fluid. Finally, the new receiver configurations have a lower overall optical intercept region resulting in a higher geometric concentration ratio for the receiver. Compared to the base case analysis (flat plate receiver), the novel tubular geometries results showed an increase in thermal efficiency.

1. INTRODUCTION

Externally configured CSP central power tower receivers have been extensively studied in simulations and experiments. The external receiver configuration is a common form for CSP towers and has been the focus of many studies and experiments. The main studies for proving this technology was performed at the Solar One and Solar Two pilot projects. Solar Two has quickly become the "standard" for molten salt power towers and its receiver was an external, cylindrical receiver. This receiver

was composed of many tubes that formed flat panels which were arranged in a cylindrical configuration. This receiver was proven to have thermal efficiencies of up to 88% [1] on multiple occasions. Typical molten salt receivers are "flat" panels, composed of tubes, arranged in some formation such as the Solar Two receiver (cylinder geometry). The current SunShot initiative requires a thermal efficiency of greater than 90% [2] which was not obtained at Solar Two. New advances in receiver design must be achieved in order to hit this performance metric. One way to do this is to manipulate the receiver geometries in order to increase thermal efficiency by reducing radiative heat loss from the system. A recent report by Garbrecht et al. showed that the use of pyramidal structures could reduce reflective loses by 1.3% [3]. The disadvantage of the pyramid structures were hot spots at the peaks of the structures due to low flow conditions. An analysis report by Rocketdyne in 1974 initially evaluated some star receiver geometry concepts [4]. The findings in this report showed that although there were some advantages in the star receiver geometries, there were less complications in the engineering design for a cylindrical receiver. However, the thermal efficiency advantages of the receivers were not fully evaluated, but was stated that the question of surface solar absorptivity could be impactful on design choices. In a cylindrical design, most of the reflected and thermally emitted radiation is returned to the environment resulting in a view factor close to 1. There is a slight cavity effect between tubes, and studying the advantages of increasing this effect is studied in this work. If the receiver panels were arranged in a way to take advantage of lower external view factors some of the reflected and thermally emitted radiation can be "re-captured" by the panels that "see" one-another. Sandia National Laboratories (SNL) has invented [5] a series of receiver designs in order to take advantage of lower external view factors which should increase thermal efficiency of external, tubular receivers.

2. PREVIOUS WORK

Computational fluid dynamics (CFD) models were created to replicate the Solar Two receiver and to verify experimental results seen at the pilot plant. Christian et al. [6] verified that CFD can be used to evaluate thermal losses from an external receiver when compared to experimental results. This information has led to confidence in using CFD to look at alternative receiver designs and evaluate how they should perform under some operating conditions.

Initial work at SNL for alternative receiver designs focused on comparing different receiver geometries to the base case study of a cylindrical receiver design (Solar Two) (see Figure 1 for alternative receiver designs). Note that the receiver base case changed within this study to a flat plate geometry due to the anticipated experimental efforts at the NSTTF. CFD analysis was performed on several different receiver geometries to determine impacts on thermal efficiencies. These receiver designs had the same exposed surface area and a constant temperature applied to the surface while evaluating radiation, natural convection, and forced convection (wind speed of 7 m/s). The constant temperature condition was a first-cut, quick modeling effort to understand if receiver geometries could impact efficiency significantly. Results presented in [7] detail the initial work that shows a thermal efficiency increase of close to 10% is possible with these alternative designs (see Figure 2).

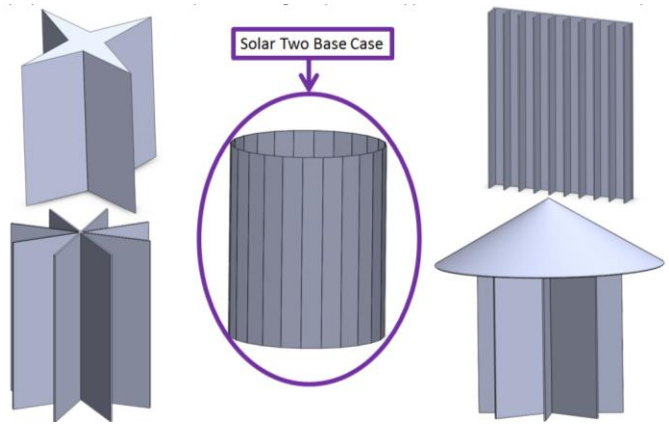

Figure 1. Initial receiver design concepts for comparison to a base-case cylindrical receiver [5]

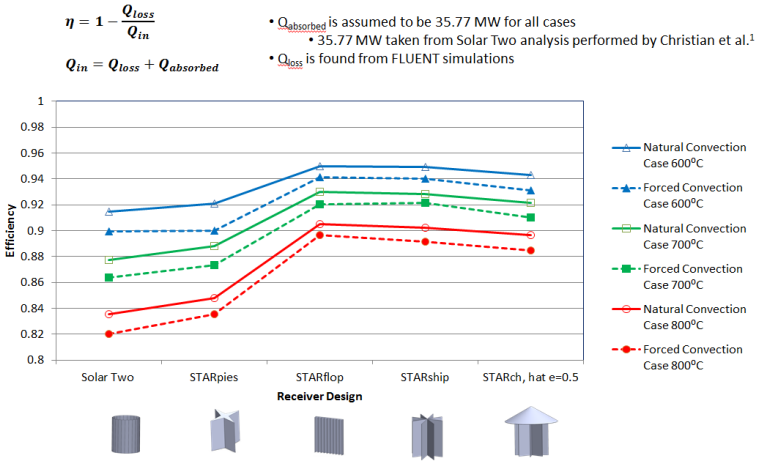

Figure 2. Receiver thermal efficiencies with three different temperature inputs and evaluating natural and forced convection effects.

The work in [7] concluded that varying receiver designs can impact thermal efficiency of a receiver. However, a more rigorous modeling and experimental analysis must be performed. The work of this project is meant to fully validate the advantages of new receiver designs. The receiver geometries changed for following work due to anticipations to perform experimental work. The new receiver designs were designed such that they would be easier to fabricate and test at

the NSTTF (north-facing receivers). The new receiver geometries can be seen in Table 1.

3. CURRENT METHODOLOGY

3.1. Technical Objectives

The results from the previous analyses were taken and applied to a more rigorous suite of simulations to evaluate the impact that each factor of the design can have on thermal efficiency of the receiver. Three technical objectives (TO) served as a guideline for creating and evaluating receiver designs:

1. Increase the light trapping and effective solar absorptance of the receiver by adding radial or linear structures
2. Reduce the thermal emittance of the receiver by taking advantage of local view factors in the hottest regions of the receiver
3. Increase the thermal efficiency of the receiver by increasing concentration ratio of the receiver through the use of a smaller overall aperture size (optical intercept) while maintaining the same exposed surface area and power

The main focus of this paper is on TO 3 while the other objectives will be commented on.

Spillage is currently not considered for this work. The focus is to first identify if it is possible for these different receiver geometries to achieve higher thermal efficiencies. As the receiver designs progress and show increased efficiencies, further engineering efforts will account for and minimize spillage losses and consider other important engineering issues such as structural stability and cost.

3.2. Receiver Geometries

Several receiver designs were created and assumed to be installed at the NSTTF tower which dictates the receiver to be a north-facing configuration. The base case receiver design was changed to a flat plate receiver from a cylindrical design for this purpose. A prototype receiver is planned for fabrication and installation for experimental validation at the NSTTF.

Four receiver designs are analyzed in this work and are displayed in Table 1. The rectangular flat plate receiver serves as the base case receiver. The external view factor for this receiver is 1. Since testing is expected to commence at the NSTTF for this work a cylindrical receiver (original base case was deemed inappropriate and a flat plate receiver is easier to build for testing purposes). The radial fin receiver is a vertically oriented circular receiver base with fins aligned vertically at set points along the curvature. The linear vertical finned receiver is a flat base with vertical fins along the height. Finally, the horizontal slate finned receiver is a linear design with fins that run horizontally across a base plate, but are slanted downwards towards the heliostat field. In all of the finned cases, it is assumed that the receiver heat transfer fluid is running through the fins. Each of the receiver designs has the same exposed surface area of 4 m^2. Each fin will be irradiated on both sides and headers will be considered in later analysis.

Table 1. Receiver designs [5]

Base Case Study-Flat Plate Receiver; Height = 2 m; Width = 2 m; Exposed Surface Area = 4m^2	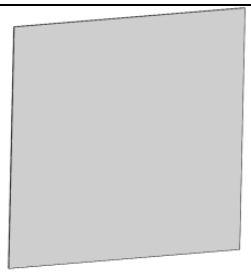
Radial Finned Receiver; Height = 1.5 m; Width = 1 m; Exposed Surface Area = 4m^2; Fin length = 0.4 m	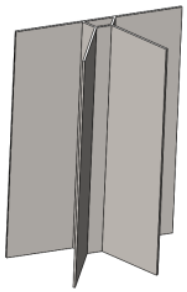
Linear Vertical Fin Receiver; Height = 0.95 m; Width = 1 m; Exposed Surface Area = 4m^2; Fin length = 0.4 m	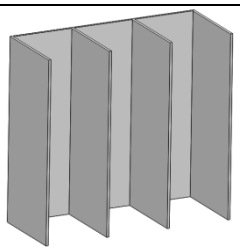
Horizontal Slate Fin Receiver; Height = 0.84 m; Width = 1 m; Exposed Surface Area = 4m^2; Fin length = 0.4 m	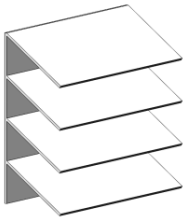

3.3. Modeling Approach

A specific modeling approach was devised to achieve the goals for Technical Objective 3. The metrics for evaluation are heat loss and surface temperatures. The best receiver will have a high thermal efficiency, while maintaining feasible surface temperatures for the materials chosen. Three stages are necessary to properly evaluate receiver designs for best thermal efficiencies. The stages are:

1. The receiver geometries were created to have the same exposed surface areas, but with differing optical intercept areas (TO 3) (Work performed in this paper)

    a. A uniform flux on the boundary was initially used to evaluate losses
    b. A ray trace analysis was used to simulate flux distributions and to achieve the same amount of power on the receiver within the smaller intercept region
2. The geometries are taken and modified to increase the light trapping effects of the receiver (TO 1)
    a. The orientation, size, and number of the fins were modified to achieve a good flux distribution
        i. Not all of these geometries were run through FLUENT due to the amount of runs, but were down selected based on the results of ray tracing
3. The best performing geometry after stage 2 of modeling will be evaluated with differing flow patterns to achieve TO 2

This paper focuses on stage 1 which achieves TO 3 while two other stages will be future work.

4. MODELING

In modeling TO 3, it should be noted that the other technical objectives are being separated out from the results from this first objective.

Ray tracing is performed in this stage of modeling, but the incident power on each receiver geometry is scaled to be identical across all cases. In doing this, light trapping advantages of the finned structures are not taken into account. This causes the first technical objective to focus only on the increased geometric concentration ratio advantage of each receiver geometry. As the power on the receiver is scaled, the flux densities are also increased on the receivers with the smaller optical intercept areas. This increase of flux magnitude on the receivers is an advantage of the increased geometric concentration ratio which results in higher thermal efficiencies.

4.1. Stage 1 Model Setup

The four receiver geometries have the same exposed surface area of 4 m^2. The base plate model is the largest footprint receiver as it occupies a 2 m x 2 m space. The other receiver designs are 1 m wide while the height varies to achieve the same surface area goal. The smaller footprint of the alternative receiver designs has the ability to have a higher flux concentration with the same amount of incident power (ray traces were performed for the NSTTF to get the proper flux distributions). The receiver walls were 3.175 mm thick. This wall thickness was deemed appropriate based on receiver structural studies containing a high temperature and high pressure super-critical carbon dioxide heat transfer fluid. During the modeling process, the flux boundary conditions were imposed on the external face of the receiver walls while a heat sink boundary condition is applied on the internal walls of the receiver. The receiver walls had material properties of Haynes 230 with an average thermal conductivity of 19.4 W/m-K, specific heat of 507 J/kg-K, and density of 8970 kg/m^3. These are properties for the material at ~600°C.

Two flux heating boundary conditions (BC) were explored for this stage of the modeling process. The first heating BC was using a uniform heat flux on the exposed surface of the receiver. The exposed surface is composed of the faces of the receiver which could see flux from the heliostat field. This heating condition was used to verify that the model was running properly and also evaluates if the natural convection of the receivers is critical when heated uniformly. The uniform flux heating condition does not properly explore TO 3. The objective of TO 3 is to evaluate the smaller optical intercept area which increases the geometric concentration ratio of the receiver. The incident power remains the same, but now the power is incident on a much smaller optical intercept area (4 m^2 vs. 0.84 m^2 for the smallest receiver optical intercept area). The proper way to evaluate this boundary condition is to run a ray trace simulation to evaluate the flux distribution on the receiver. In all cases, the incident power on the receiver is 2 MW_t based on power available at the NSTTF. The NSTTF can generate 6 MW_t, but 2 MW_t is achievable on a smaller receiver which is easier to fabricate and test for future studies.

Two ray trace objectives and flux patterns were evaluated. The first objective was using a single aim point heliostat pattern. Each receiver had a single aim point at the center of the receiver resulting in a flux pattern with the maximum flux at the center of the receiver and decreases towards the edges of the receiver. The second objective was trying to spread the incident power on the receiver as uniform as possible using multiple aim points. This does not result in the perfect uniform flux condition imposed initially, but matches closely to what would be seen if the receiver would be in operation at the NSTTF. The resulting heat losses are representative of what happens when a receiver has a smaller optical intercept area. The ray trace process is described in detail in section 4.2.

The heat flux incident on the receiver is applied as a "heat generation rate" in FLUENT. This is required when modeling an external domain around the receiver. The external domain around the receiver is required to include the effects of convection cooling on the receiver external surface. The external domain is made big enough to verify that its size does not interfere with the solution results.

In all of these studies there was no fluid flow in the receiver. The receiver had an internal wall with a constant temperature to act as a heat sink. A 600°C temperature condition was applied to all internal walls that were exposed to an external heat flux condition. This is an approximation of a fluid at this temperature in the receiver removing heat from the system. This simplification was made for this first round of modeling, and future modeling will include an actual heat

transfer fluid to more accurately predict temperature distributions on the receiver surfaces.

The Discrete Ordinates (DO) radiation model (5 x 5 divisions; 3 x 3 pixels) in Fluent was utilized. The k-ω SST turbulence model was turned on for these studies since the boundary layer at the receiver may have turbulent features as the walls are heated. A grid independence study was performed to verify that the solution was mesh-independent.

4.2. Ray Trace Flux Distributions

SolTrace is free ray-trace software available through NREL. SolTrace is specifically designed to model CSP applications. Sandia has developed a software code to take a CAD geometry, import it into SolTrace, then export the flux data into FLUENT as a heat boundary condition. Each ray trace simulation can have anywhere from 10-100 million rays incident on the receiver depending on the accuracy of the ray trace required. In this work, 10 million rays were shown to give consistent flux distributions required for the CFD modeling. Each receiver was evaluated with a single aim point and then with multiple aim points to achieve a more distributed flux on the receiver. At this point, an optimized ray trace for a distributed flux has not been explored.

4.2.1. Aim Points

The single aim point flux distributions can be seen in Table 2. These contour maps of the flux show how the heat flux magnitudes differ on the different receiver geometries. The highest flux values are seen in the Horizontal Slate Fin receiver. This is due to the fact that the receiver height is much smaller than 2 m and width is only 1 m. In addition, most of the power is incident on the back faces and not on the fins themselves leading to much higher flux values on the back walls. These flux maps show how a reduced optical intercept area impacts the "hot" regions on smaller optical intercept receiver designs. There is a significant increase in geometric concentration ratio on some of the designs resulting in more power in a smaller optical aperture area (currently neglecting spillage).

An important observation is that these receiver concepts are meant to be tested at the NSTTF. However, the flux maps shown in Table 2 show that the peak flux for the base case receiver is about 1300 suns while the peak flux for the horizontal fin receiver is about 2500 suns. This is achievable at the NSTTF through the use of focusing less or more heliostats at the single aim point. Each receiver has an incident total power of 2 MW, but the difference in flux levels is achieved due to the receiver sizes. The base case receiver is larger which allows more power from less heliostats to be absorbed such that the peak flux levels remain fairly low, but still achieving the 2 MW power requirement. The other receiver designs are much smaller (due to the increased geometric concentration ratio) such that more heliostats are allowed to be focused on the single aim point while still having the same incident power on the receiver. This result would be due to the spillage effects at the NSTTF with smaller receiver geometries.

A multiple aim point strategy was employed to spread the flux from the field over the receiver surfaces. Four aim points were utilized by splitting the geometry into equidistant points from the outer edges of the receiver geometry. The multiple aim point flux distributions are seen in Table 2 (Note: To see the flux distributions the color scales for each receiver are different). These flux patterns are quantitative patterns of the 2 MW incident power on the receiver. Each of the flux patterns seen is with four aim points that are evenly distributed across the optical aperture of the receiver (see Figure 3 for example aim point distribution) in an attempt to create a uniform flux on the receiver resulting in a flux magnitude reduction. This is most dramatically seen with the base case receiver geometry, but is prevalent in all of the receiver designs. However, the more uniform flux maps creates a more evenly heated heat transfer fluid and creates less thermal strain on the receiver walls which is highly desirable in actual plants.

An interesting observation arises for the linear vertical fin receiver (row 3 in Table 2). The flux distribution is greatest at the bottom of the receiver. This is caused by the directionality of the heliostat beam and arrangement of the fins. The beam is incident on the receiver with an upward direction and converging towards the center of the receiver. The vertical fins block the beam from reaching the middle of the receiver such that the flux distribution is highest at the bottom of the receiver.

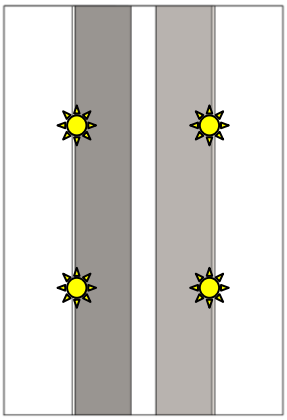

Figure 3. Example aim point pattern on the radial finned receiver for the multiple aim point ray traces; Sun symbols represent the aim points

These ray trace data sets were imported into FLUENT and run through CFD to determine the impacts on heat loss of the systems. The ray trace data was included as a "profile" on the external walls of the receiver. Discrete flux values are applied according to receiver coordinates and then FLUENT interpolates between the nodes for any spaces without known flux values. Due to the external domain boundary to account for natural convection, the heat fluxes had to be applied as a heat generation rate. The wall that the heat flux is applied to is

a coupled wall between the wall thickness and the external domain. The heat generation rate is shared between the coupled wall, but the total heat flux is still applied to that boundary.

5. RESULTS AND DISCUSSION

The receiver geometries were created to have the same exposed surface areas, but with differing optical intercept areas (TO 3). A uniform flux model and a distributed flux model were used to evaluate the effectiveness of a smaller optical intercept. The uniform flux modeling looks at losses based on truly even heating of the receiver. The distributed flux modeling evaluates a more realistic heating of the receiver.

5.1. Uniform Flux Modeling

A uniform flux, resulting in 2 MW incident power on the receiver surfaces was modeled to evaluate the heat transfer between the receiver geometries. A uniform flux (500 kW/m^2 for all receivers) greatly simplifies the problem and the resulting radiation and convection losses from the receivers are nearly the same for all cases. This modeling result does show that if a truly uniform flux distribution is achieved then the differing receiver shapes can have an impact of up to 4.5% on the thermal efficiency of the receiver. However, a distributed flux boundary is anticipated which could result in higher gains in thermal efficiencies. The distributed flux modeling results are shown in section 5.2.

Figure 4 displays the thermal efficiencies and radiation and convection heat losses as a total percentage of power on the receiver. The Base Case receiver has the lowest thermal efficiency due to a higher radiation heat loss. The other receiver geometries have internal view factors between the finned structures which reduce the amount of radiation losses from the systems. The Horizontal Slate Finned receiver has the highest thermal efficiency of 95.6%. The horizontal fins aid in reducing convective heat loss from the receiver. Radiation heat loss is also reduced due to the arrangement of the fin structures.

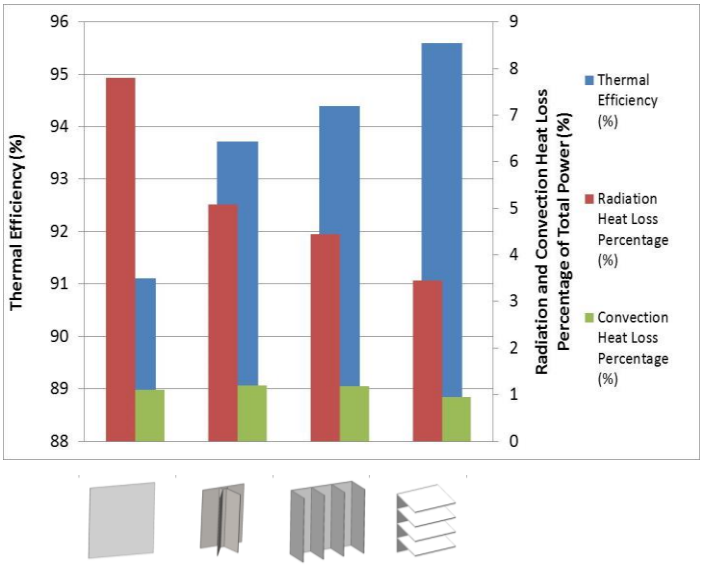

Figure 4. Uniform heat flux on receiver thermal efficiency, radiation heat loss percentage of total heat input, and convection heat loss percentage of total heat input for the different receiver geometries

5.2. Distributed Flux Modeling

The receivers were evaluated with a multiple aim point flux distribution and a four aim point flux distribution. The single aim point flux studies have a single region of high fluxes whereas the four aim point flux studies have the single high flux region spread more evenly across the receiver.

It is clearly seen in Figure 5 and Figure 6 that there is a clear difference in thermal efficiencies between the geometries. The lowest thermal efficiency is the base case scenario while the highest is the Horizontal Slate Fin receiver design. The radiative losses are decreased with the finned receiver designs.

Table 2. Flux distributions shown in FLUENT for single aim point and multiple aim points (Note the change of color scale for flux patterns)

Geometry	Single Aim Point (W/m^2)	Four Aim Points (W/m^2)
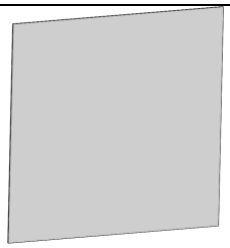	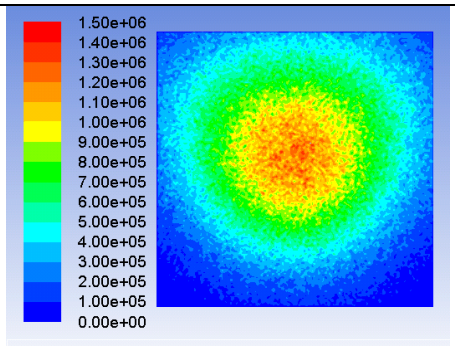	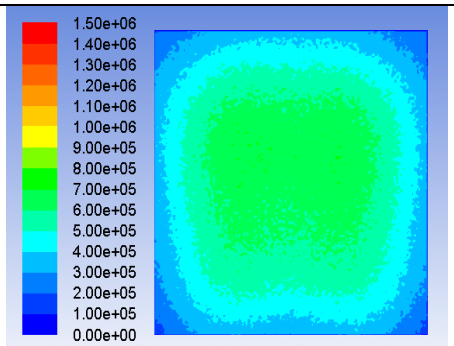
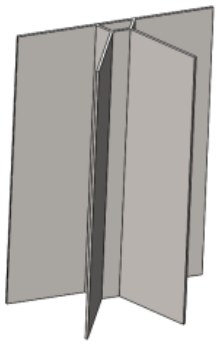	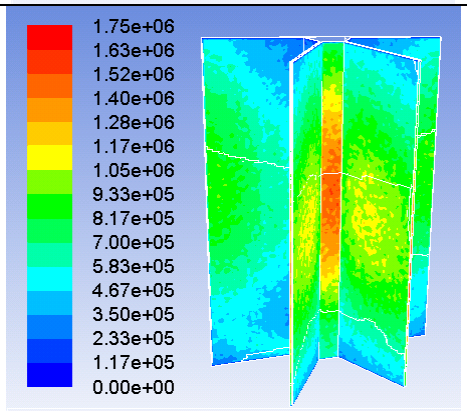	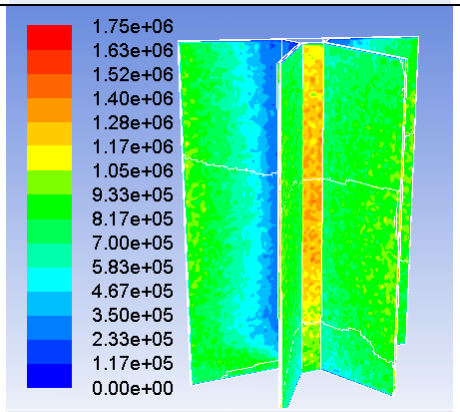
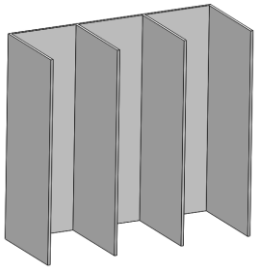	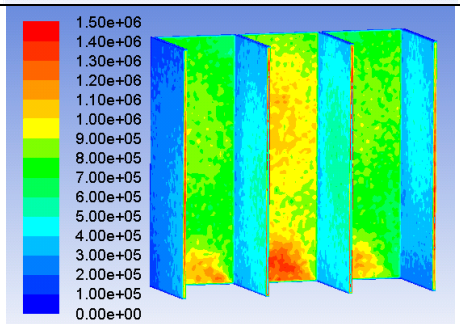	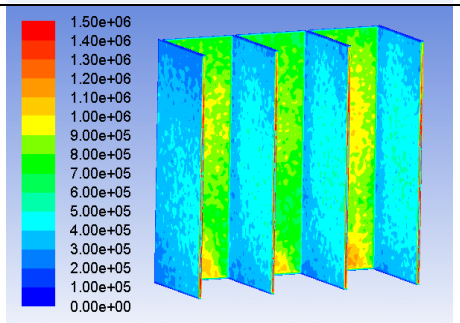
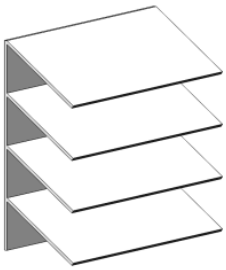	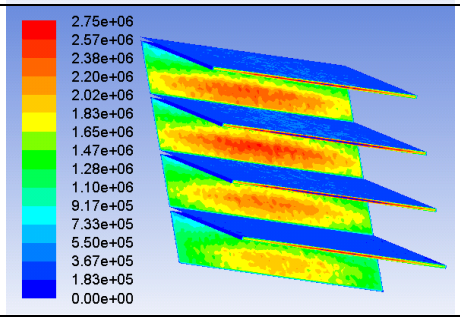	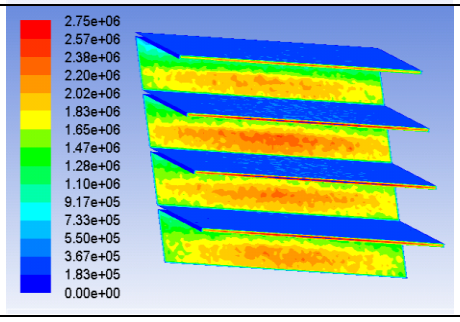

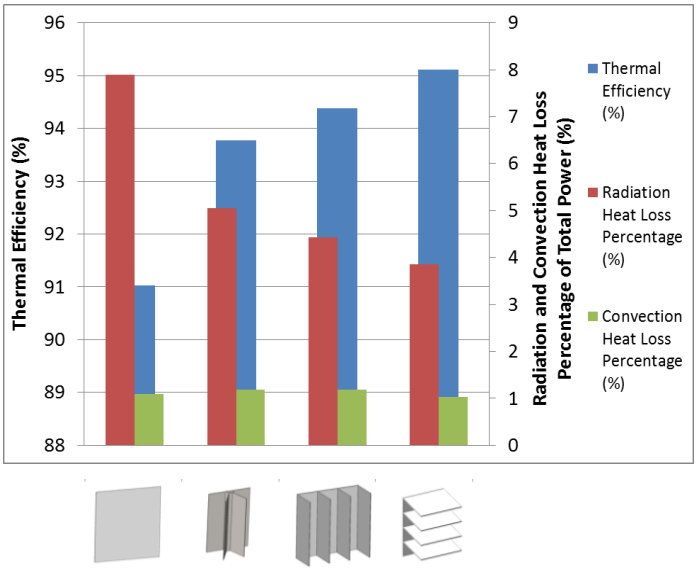

Figure 5. Single aim point ray traces thermal efficiency, radiation heat loss percentage of total heat input, and convection heat loss percentage of total heat input for the different receiver geometries

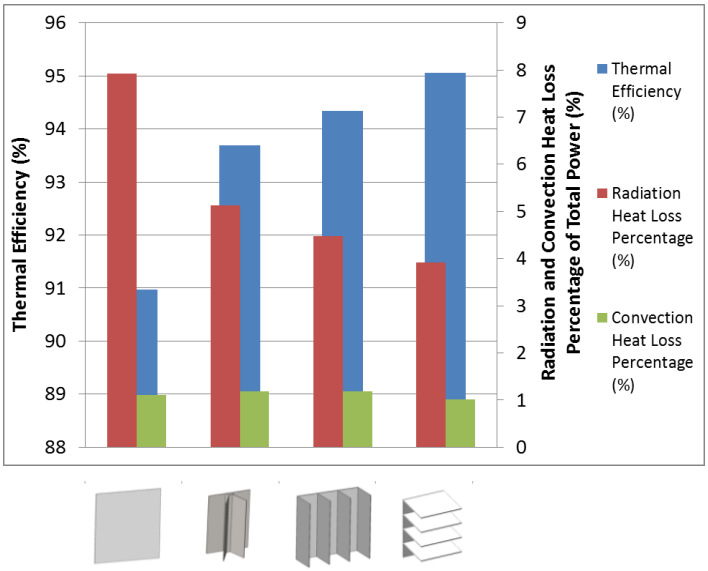

Figure 6. Four aim point ray traces thermal efficiency, radiation heat loss percentage of total heat input, and convection heat loss percentage of total heat input for the different receiver geometries

However, it must be noted that when comparing the uniform flux cases with the single and four aim point flux distributions, that the average wall temperature values for all geometries are nearly identical. This is due to the heat sink simplified boundary condition. In the ray trace studies, some of the surfaces don't have high fluxes present but the walls in these regions reach 600°C because of the heat sink boundary condition. This results in average wall temperatures between all cases which are nearly identical. The ray trace studies result in temperature distributions, but some receiver spots have low radiation losses while others at higher temperatures have increased radiation losses. Overall, the surface temperatures average out to be nearly the same for all cases resulting in very similar thermal efficiencies across all cases of the uniform flux results and the distributed flux results.

and Table 3 show the front wall temperatures contour plots of the receiver geometries and the maximum and average wall temperatures.

Table 3. Receiver front surface temperatures (K)

Geometry	Max. Temp. (K) Uniform Flux	Max. Temp. (K) Single Aim Point Flux	Average Temp. (K) Uniform Flux	Average Temp. (K) Single Aim Point Flux
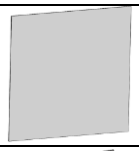	943.0	1048.7	941.1	939.8
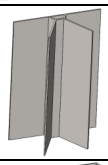	990.0	1197.7	939.7	938.9
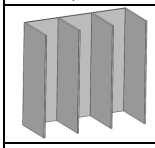	990.5	1257.2	944.6	945.4
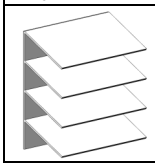	991.6	1469.6	945.6	943.5

The next step in the modelling process is to use an actual heat transfer fluid instead of the constant temperature heat sink boundary condition. It is believed that the differences between models will clearly be seen in these cases due to the non-uniformly heated fluid.

Table 4. Wall temperatures of the receiver geometries, (Note the scale between the uniform flux and single aim point temperature contour plots are different) (The white lines in the figures represent the outlines of the receiver geometry and in some cases the mesh partitions for the parallel solver.)

Geometry	Uniform Flux Temperatures (K)	Single Aim Point Temperatures (K)
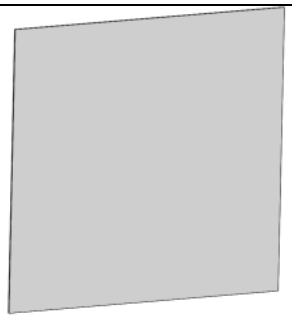	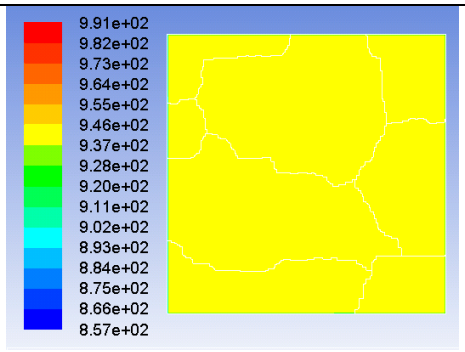	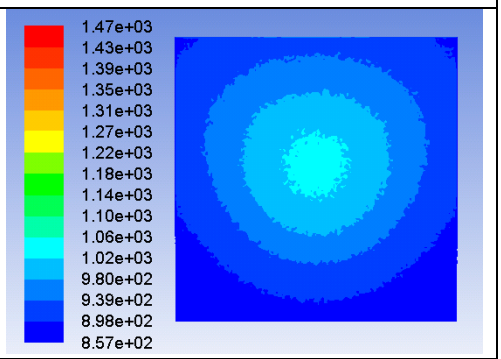
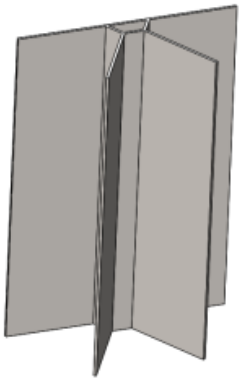	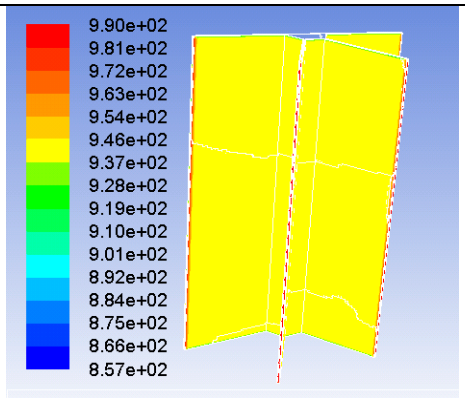	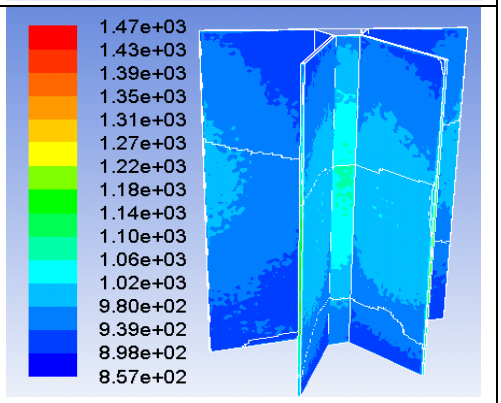
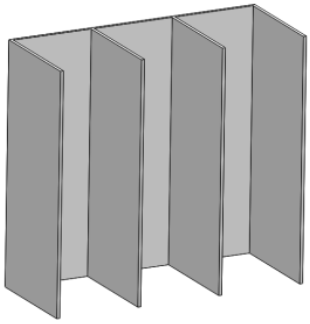	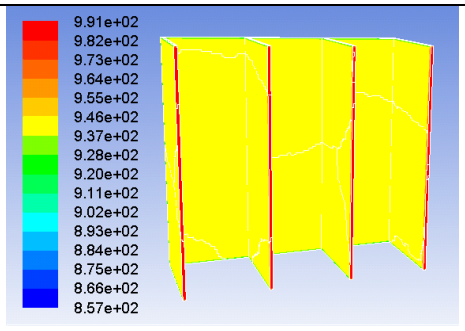	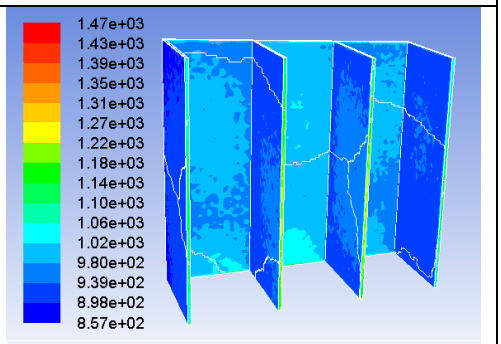
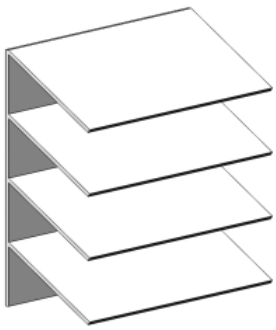	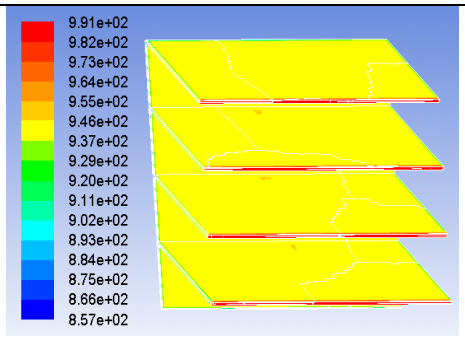	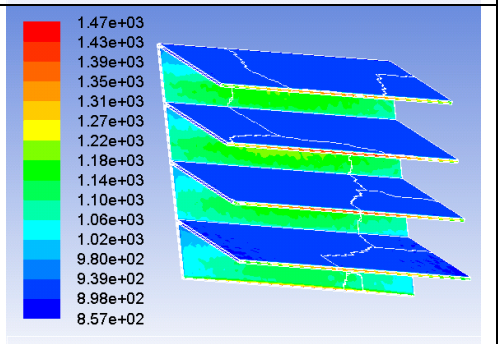

6. CONCLUSIONS

Four receiver geometries were compared to evaluate the effect on thermal efficiency due to geometric differences. Each receiver had a different optical intercept area which results in a higher geometric concentration ratio for the smaller receivers. The base case scenario is a rectangular plate and in all cases resulted in the lowest thermal efficiency. The Horizontal Slate Fin receiver had the highest thermal efficiency with 95.5% and was a 4.5% increase over the flat plate geometry. A trend can be clearly seen as finned structures are added onto the receiver. Radiation losses go down with the increase in geometric concentration ratio and addition of finned structures.

Previous results, shown in Figure 2, show initial receiver designs modeled at constant wall temperatures. For the 700°C, natural convection cases the increase in thermal efficiency of the finned structures versus the standard cylindrical receiver design reached an increase of nearly 4%. These results are consistent with the results seen in this study.

A heat sink boundary condition can provide results that show the relative performance of each receiver, but are deemed to not accurately portray an actual CSP plant receiver. A heat transfer fluid must be modeled to more accurately capture the effects on non-uniform heating on the receiver and the fluid. The heat sink results in average temperatures that are nearly identical between the uniform flux cases and the distributed flux cases. The next round of modeling will include the heat transfer fluid in the simulations.

7. ACKNOWLEDGMENTS

Sandia National Laboratories is a multi-program laboratory managed and operated by Sandia Corporation, a wholly owned subsidiary of Lockheed Martin Corporation, for the U.S. Department of Energy's National Nuclear Security Administration under contract DE-AC04-94AL85000. The United States Government retains and the publisher, by accepting the article for publication, acknowledges that the United States Government retains a non-exclusive, paid-up, irrevocable, world-wide license to publish or reproduce the published form of this manuscript, or allow others to do so, for United States Government purposes.

8. REFERENCES

[1] Pacheco, J. E., 2002, "Final Test and Evaluation Results from the Solar Two Project," SAND2002-0120, Sandia National Laboratories.

[2] Energy, U. S. D. o., 2011, "SunShot Initiative."

[3] Garbrecht, O., Al-Sibai, F., Kneer, R., and Wieghardt, K., 2013, "CFD-simulation of a new receiver design for a molten salt solar power tower," Solar Energy(90), pp. 94-106.

[4] Friefield, J. M., and Friedman, J., 1974, "Technical Report No. 1: Solar Thermal Power Systems Baded on Optical Transmission,"Rocketdyne Division, Rockwell International.

[5] "U.S. Patent Application 14535100, Filed Nov. 6, 2014, BLADED SOLAR THERMAL RECEIVERS FOR CONCENTRATING SOLAR POWER."

[6] Christian, J., and Ho, C., 2012, "CFD Simulation and Heat Loss Analysis of the Solar Two Power Tower Receiver," ASME 2012 Energy Sustainability and Fuel Cell ConferenceSan Diego, CA.

[7] Ho, C., Christian, J., Ortega, J., Yellowhair, J., Mosquera, M., and Andraka, C., 2014, "Reduction of radiative heat losses for solar thermal receivers," SPIE Optics and Photonics for Sustainable EnergySan Diego, CA.

